Twenty-Fifth Symposium (International) on Combustion/The Combustion Institute, 1994/pp. 569–576

ON THE COMBUSTION OF WOOD-CHAR SPHERES IN O_2/N_2 MIXTURES—EXPERIMENTS AND ANALYSIS

S. DASAPPA AND H. V. SRIDHAR
ASTRA
Indian Institute of Science
Bangalore 560 012, India

P. J. PAUL AND H. S. MUKUNDA
Department of Aerospace-Engineering
Indian Institute of Science
Bangalore 560 012, India

U. SHRINIVASA
Department of Mechanical Engineering
Indian Institute of Science
Bangalore 560 012, India

This paper discusses the results from experiments and analyses of the combustion of wood-char spheres for varying O_2 in an O_2-N_2 mixture. The experiments show that for particle diameters (d_0) in the range 2–15 mm, the char burn time (t_b) in air is given by $t_b \sim d_0^{1.87}$ at 300 K. At higher ambient temperatures, the exponent on d_0 goes up to 2.0. The results at reduced oxygen fraction show extinction at partial conversion and zero conversion at oxygen mass fractions less than 0.14 at an ambient temperature of 300 K. Regarding flow effects, for Reynolds number (Re) more than 500, conversion is only partially complete for runs at 300 K. The mathematical model consists of a spherically symmetric porous body undergoing heterogeneous conversion with finite-rate chemistry and associated diffusion into the pores. Free and forced convective heat and mass transfer effects outside the sphere are approximately modeled. The results show a near complete agreement on most aspects. The extinction at low ambient oxygen fraction and the extinction after partial conversion at low oxygen fractions or in presence of forced convection are argued to be due to the process of becoming statically unstable. The results of lower ambient oxygen limit, also observed in some sparsely conducted experiments, apparently have implications in planetary evolution studies.

Introduction

Wood-char combustion with O_2/N_2 mixtures is of importance in several industrial processes, more particularly in wood gasifiers, where one of the active processes is the oxidation of carbon at reduced oxygen fractions. A review on gasification of coal char is given by Laureandeau [1]. Earlier, Mukunda et al. [2] studied single wood-sphere combustion, including that of the char. The model included diffusion and reaction in the pores and char conversion times slightly under those predicted from experiments. The predicted core temperatures ranged between 1600 and 1650 K. The experiments of Kuwata et al. [3] and experiments conducted here have shown temperatures with a maximum of 1000 K. The model used in Ref. 2 contained a C-O_2 reaction alone, and the reaction of C-CO_2, likely to be important at high temperatures, was neglected. Also, in a gasifier operation, the possibility of reactions of char at reduced oxygen concentrations exists. The number of explorations into such effects in the literature seems limited [4,5].

The present work has been undertaken to obtain more detailed experimental data on the weight loss, the core and surface temperatures with time, extinction, and related features at reduced oxygen fraction; and the flow effects on wood-char spheres between 2- and 25-mm diameter, a range of interest in wood gasifiers. A computational analysis of the process is also made, to understand the physics of char combustion and to bring out the controlling processes at various regimes of combustion.

The Experiments

The experimental setup consists of a quartz reactor 40-mm in diameter placed in a temperature-controlled furnace [6]. For high-temperature runs, the reactant gas is preheated to the furnace temperature by letting the gas pass through a helical quartz tube

wound around the reactor. The flow rate of the gas is measured using a capillary flowmeter. Air or a mixture of oxygen and nitrogen is used depending upon the requirements. In the latter case, flow rates of O_2 and N_2 are measured before mixing and being led into the reactor. The oxygen fraction is further checked by a gas analysis of the mixture.

The char samples of size 2.0–15 mm are prepared either by burning dried wood spheres (*Ficus*) in air and quenching them at the end of flaming combustion or by heating them slowly in an inert environment. The density of char obtained by the former method is 180 ± 20 kg/m^3, and the latter method is 400 ± 30 kg/m^3. Density of the char is calculated from the weight of the char sphere and the volume obtained by measuring the diameter. The diameter is averaged over measurements on many locations on the sphere. The charcoal spheres obtained are repeatedly dried in an oven at 373 K and cooled in a desiccator a few times before use. In some cases, the char samples obtained at the end of the pyrolysis process are nonspherical and are shaped by filing to true spheres.

Porosity is obtained from the apparent density of the porous char and the solid char by the relation $\varepsilon = (1 - \bar{\rho}/\rho_c)$. This value is verified in a few cases by the water absorption technique. A dried sample is dipped in water and allowed to soak for a few hours. After removal, the sample is weighed. The difference in the initial weight before soaking and the final weight after soaking gives the amount of water absorbed. This would give the void fraction in the porous char, which is the porosity of the given char sample.

The sample was suspended, using a fine wire basket, from a balance and heated using a spirit lamp flame enclosing the entire sphere so that oxidation of char is prevented and the temperature of the char is increased to 900 K. The sample was then placed inside the reactor maintained at the required temperature, and the reactant gas was passed through the reactor. The total conversion time and the flow rate of the reactant were noted. During the experiments at low Re (<50), it was observed that the diameter of the char sphere was gradually decreasing with the ash layer covering the sphere. However, the carbon core was visible through the ash layer till the end of the burn time. For runs with air at 300 K, conversion could not be initiated below a diameter of 2 mm. With varying O_2 fraction, ($Y_{O_{2,\infty}}$) below 0.14, the char particle quenched after introduction into the reactor. This phenomenon was found similar for different diameters in the range of 4–14 mm. The conversion was found incomplete for $Y_{O_{2,\infty}} < 0.21$. In these experiments, it was ensured that flow effects did not influence the results by keeping Re < 30. Experiments on the effect of flow velocity were conducted by varying the flow rate of air into the reactor, thus changing Re. It was found that for Re > 500, the conversion was incomplete, with a weight loss of about 60–95% depending upon the mass fraction of oxygen. Also, it was noticed that the ash was getting blown off from the surface in most such cases. Experiments were also conducted to determine the core temperature by inserting a 100-μm Pt-Pt 13% Rh thermocouple at the center of a wood sphere undergoing combustion. During this period, the temperature was monitored, and it never exceeded 950 K.

The Model

The processes taking place during the combustion or gasification of porous carbon spheres are the diffusion and convection of the species and energy in the porous medium and the heterogeneous reaction between the gaseous species and the char. These are modeled in the present analysis using the unsteady spherically symmetric one-dimensional conservation equations. The conservation equations are

$$\frac{\partial}{\partial t}(\rho\varepsilon Y_i) = \frac{1}{r^2}\frac{\partial}{\partial r} \cdot\left(-\rho v r^2 Y_i + r^2 \bar{D}\rho \frac{\partial}{\partial r} Y_i\right) + \dot{\omega}_i''' \tag{1}$$

$$\frac{\partial \varepsilon}{\partial t} = \frac{-\dot{\omega}_c'''}{\rho_c} \tag{2}$$

$$\frac{\partial}{\partial t}(\bar{\rho} c_p T) = \frac{1}{r^2}\frac{\partial}{\partial r} \cdot\left(-\rho v r^2 c_p T + r^2 k \frac{\partial T}{\partial r}\right) - H_c \dot{\omega}_c''' \tag{3}$$

where $\bar{\rho} = \rho_c(1 - \varepsilon) + \rho\varepsilon$ is the average density of porous char, ρ_c is nonporous char density, ε is the porosity of the char, and $\dot{\omega}_c'''$ is the volumetric reaction rate of char with O_2 and CO_2, including the contribution due to growing of pores.

$$\dot{\omega}_c''' = \dot{\omega}_{c_{O_2}}''' + \dot{\omega}_{c_{CO_2}}''' . \tag{4}$$

The subscripts i = 1, 2, and 3 refer to species CO, CO_2, and N_2, respectively.

The volumetric reaction rate is related to the heterogeneous reaction rate per unit surface area by

$$\dot{\omega}_c''' = \dot{\omega}_c'' S_g \rho_{ap} \tag{5}$$

where ρ_{ap} is the apparent density of the char and S_g

is the surface area per unit volume of the char, which is given by Howard [7], as $S_g \rho_{ap} = 2\varepsilon/r_p$.

The surface reaction rate of carbon with oxygen is given by Howard:

$$\dot{\omega}''_{c_{O_2}} = -\frac{M_c S_1 S_2 X_{OS}}{(S_1 X_{Os} + S_2)} \tag{6}$$

where X_{Os} is the mole fraction of oxygen at the surface and S_1 and S_2 are the rate constants for absorption and desorption, respectively, given by

$$S_1 = A_c P \exp\left(\frac{-E_1}{RT}\right) \Big/ (\sqrt{2\pi M_{O_2} RT}) \tag{7}$$

$$S_2 = A_f \exp\left(\frac{-E_2}{RT}\right). \tag{8}$$

Smith and Tyler [8] use a single rate expression as $R_s = 1.34 \exp(-32{,}600/RT)$ (g/cm^2 s) for coal-char particles of 22–89 μm in size, for a temperature range of 630–1812 K. The rates calculated match with that of Eq. (8), implying that the desorption process is rate limiting in their experiments.

The reaction rate of carbon with CO_2, suggested by Semechkova and Frank-Kamenetskii and referred to in Blackwood and Ingeme [9], is given by

$$\dot{\omega}'''_{c_{CO_2}} = -\frac{k_1 p_{CO_2} - k_2 p_{CO}^2}{1 + k_3 p_{CO} + k_4 p_{CO_2}}. \tag{9}$$

No gas-phase reactions are considered. The oxidation of CO is neglected because the mass fraction of CO inside the sphere during the reaction process is too low to contribute toward any heat release.

The diffusion process are modeled after Howard [7] and discussed in our earlier work [2,6]. The reaction rate per unit area $\dot{\omega}''_c$ is related to $\dot{\omega}'''_c$ by $\dot{\omega}'''_c = \dot{\omega}''_c 2\varepsilon/r_p$.

The details of pore treatment are the same as in Ref. 6 and are not repeated here.

Initial, Interface, and Boundary Conditions

At $t = 0$, the temperature in the sphere is set at 900 K. The precise nature of the concentration profile does not matter, as the transients die down in a small fraction of the conversion time. The interface conditions at $r = r_s$ are the continuity of heat and mass fluxes. These are as [2]

$$D_g \rho \left.\frac{\partial Y_i}{\partial r}\right|_{rs} = Q(Y_{i\infty} - Y_{iS});$$

$$k \left.\frac{\partial T}{\partial r}\right|_{rs} = c_p Q(T_\infty - T_S) - \dot{R}'' \tag{10}$$

where $\dot{R}''$ is the radiative heat flux from the surface of the sphere and

$$Q = \frac{(\rho v)_S \exp(-B_0)}{[1 - \exp(-B_0)]}, \qquad B_0 = \frac{(\rho v)_S c_p}{k\mathrm{Nu}}. \tag{11}$$

Equation (10) is obtained from the solution of spherically symmetric one-dimensional conservation equations for the gas phase [2], and the effect of free and/or forced convection is accounted for by choosing the appropriate value of the Nusselt number (Nu). Nu = 2 in the absence of either free or forced convection but increases in the presence of convection. In earlier work [2], the char sphere encountered only free convection. In the present case, with flow velocities, both will be present.

Method of Solution:

The solution calls for integration of the parabolic system of partial differential equations with the initial and boundary conditions noted above. The independent variable r is transformed into a V, defined as $V = (4/3)\pi r^3$, making the system of equations fully conservative and removing the singularity at $r = 0$. The integration of the transformed equations is carried out in the same way as in Ref. 6.

Choice of Parameters:

The choice of physical, thermodynamic, and transport properties is based on the mean char properties presented as follows:

$$\rho_c = 1900 \text{ kg/m}^3 \quad r_p(t = 0) = 50\ \mu\text{m}$$

$$c_p = 1.25 \text{ kJ/kg K}$$

$$H_c = 32.60 \text{ MJ/kg} \quad k_c = 1.85 \text{ W/m K}.$$

Rate parameters for the C + O_2 reaction are

$$A_c = 1/150 \quad E_1/R = 1700 \text{ K}$$

$$E_2/\mathrm{R} = 20{,}000 \text{ K} \quad A_f = 0.0875 \text{ moles/m}^2 \text{ s}.$$

Rate parameters for the C + CO_2 reaction are as in Ref. 6. The term k_c is the conductivity of the solid phase at temperatures of 900–1200 K. This value of k_c leads to porous char conductivity of 0.4–0.5 W/m K, which is the same as in Refs. 10,11 and accounts for conduction and radiation inside the char. The thermal conductivity of the gas phase, k_g, is calculated locally. The rate parameters used in the present study for the C + O_2 and the C + CO_2 reactions are from Howard [7] and Blackwood and Ingeme [9], respectively. The initial porosity of the wood char considered is in the range of 0.75–0.85, consistent with the present measurements as well as of

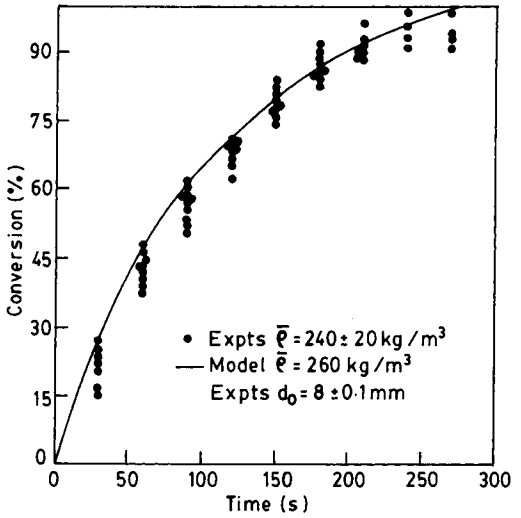

FIG. 1. The conversion with time—experiments and predictions for particle diameter of 8 mm; ambient temperature = 300 K.

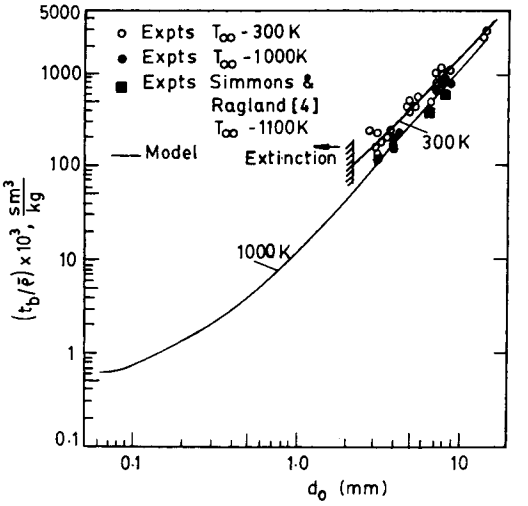

FIG. 2. Burn time for different particle diameters along with the predictions for ambient temperature of 300 and 1000 K (experimental data of Simmons and Ragland [5]).

Groeneveld and van Swaaij [12]. The initial radius of the pore is obtained from Groeneveld [13], where wood char was used for measurements. The parameters in the kinetic expression used presently are obtained from Blackwood and Ingeme. The rate of the backward reaction k_2 is obtained from the appropriate equilibrium constants. The emissivity in the expression for radiant heat loss is taken at 0.95.

Results and Discussion

Figure 1 shows the results of char conversion (x_c) with time for an 8-mm-diameter char particle at ambient condition. Char conversion is the ratio of the difference between the initial weight and the weight at any time t to the initial weight. Both experimental data and predictions from the model are presented here. The predictions compare well with the experimental data within the range of experimental error. This result would justify the choice of kinetic and transport parameters chosen for the model.

Figure 2 shows the experimental data and the prediction of burn time normalized with respect to density of char with initial char diameter for combustion in air on a log-log plot. A curve fit to these data leads to $t_b \sim d_0^{1.87}$, indicating the diffusion-dominated combustion; the departure from the $t_b \sim d_0^2$ law is due to the presence of free convection. Also shown are the experimental results for 4- and 8-mm particles in air for an ambient temperature of 1000 K. The results follow the d^2 law up to a particle size of about 1 mm. It is clear that the rise in the ambient temperature from 300 to 1000 K has raised the exponent from 1.87 to 2, because the free convection effects are very small in the latter case. Predictions in both cases seem excellent. The experiments at 300 K show extinction at a 2-mm particle size. At 1000 K, the transition from the diffusion to kinetic regime takes place in the range downward of 1 mm. Experimental results from Simmons and Ragland [5] on the combustion of char cubes are also plotted in Fig. 2, based on volume and estimated density from the available data. The burn time results of Simmons and Ragland at 1100 K are slightly lower than from the present experiments, and the predictions at 1000 K are within the experimental errors.

Predictions on the ratios of mass fraction of O_2 and CO_2 at the core to the surface are plotted with time normalized with respect to the time for full conversion at an oxidizer temperature of 1000 K in Fig. 3. In the case of the 100-μm particle, the ratio for O_2 is about 0.8, indicating that the oxygen mass fraction available at the core and the surface is nearly the same in contrast to the 400-μm particle where the ratio is about 0.3, thus switching from the kinetic to the diffusion limit. Due to the availability of O_2 throughout the particle, the ratio of CO_2 at the core to the surface is higher in the 100-μm particle compared with the 400-μm particle diameter during the burn time.

As mentioned earlier, in Ref. 2, the predicted peak core temperature was 1600–1650 K and is different from the earlier experimental data. This aspect is analyzed now. Figure 4 shows the plot of core temperature history found in the experiments and various models. The measured temperature data from this work and from Kuwata et al. [3] show clearly the peak temperature to be about 900–950 K. In earlier work

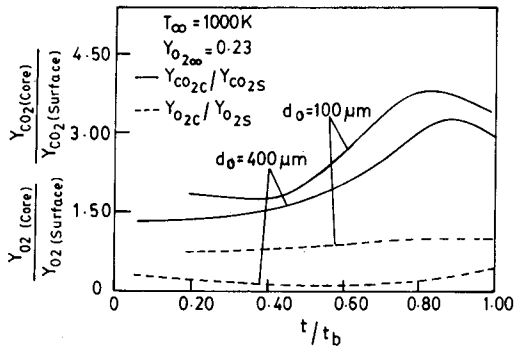

FIG. 3. Variation of the ratio of mass fractions of O_2 and CO_2 between the core and the surface for oxidizer temperature of 1000 K for an 8-mm-diameter char sphere burning in air with normalized time.

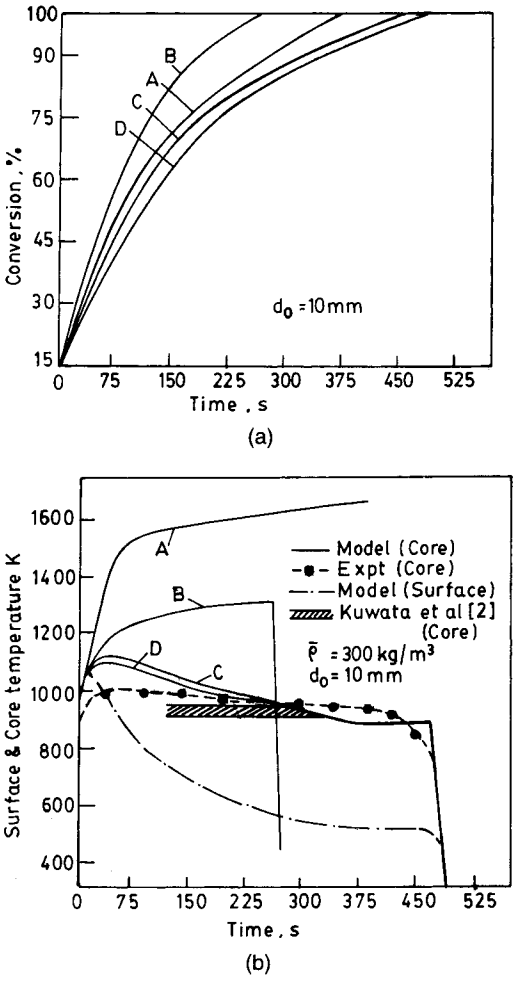

FIG. 4. Effect of the C + CO_2 reaction and thermal conduction of char on (a) conversion and (b) temperature profiles for a 10-mm-diameter char sphere burning in air. (case A: No C + CO_2 reaction and conductivity at 300 K; case B: similar to case A with addition of the C + CO_2 reaction; case C: similar to case A with thermal conductivity for high temperature; case D: similar to case C with addition of the C + CO_2 reaction).

[2] in which only the C + O_2 reaction was treated along with an equilibrium of CO and CO_2, the results showed an increase of the core temperature from 1000 K to about 1650 K toward the end (Fig. 4, curve A). As the fraction of CO_2 present inside the sphere is not small, it was argued that the endothermic CO_2-C reaction was necessary to be included. Also, the data on conductivity for red hot char showed different values [10,11]. Hence, the influence of the conductivity also is examined. The results with various options are presented as curves B, C, and D in Fig. 4. Case B indicates the results with the inclusion of the C + CO_2 reaction mechanism along with C + O_2. The effect of endothermicity is found to be significant in reducing the peak core temperature to about 1250 K. Case C concerns the effect of enhanced conductivity due to high temperature. It is seen that the conductivity plays an important role in reducing the peak core temperature to about 1150 K. Case D indicates the results with the addition of the C + CO_2 reaction to case C. The difference between cases C and D with regard to the core temperature and the conversion profile is not appreciable. It is clear that the contribution toward the reduction of core temperature is due to the conductivity of char; inclusion of the C + CO_2 reaction mechanism is not essential for a good prediction of the peak temperature in the present case.

Another aspect that needs consideration is the burn time of the particle. In case A, the burn time predicted was slightly lower than the range of the experimental results obtained, whereas in case B, where the CO_2 reaction is introduced, the burn time is reduced by about 25%, indicating the contribution from the C + CO_2 reaction. Enhanced thermal conductivity, as in case C, has increased the burn time of the particle compared to that of case B, with more heat loss from the reaction zone of the char particle to the ambient and reduction in the peak core temperature. Inclusion of the CO_2 reaction to case C has not altered the reaction time, indicating lower importance of this reaction. This result should be contrasted with case B, where the reaction time was reduced by 25% with CO_2. It is clear from these results that the contribution from the CO_2 reaction would be significant at elevated temperatures and, thus, should not be neglected. Thus, for the other cases, like the one studied by Ubhayakar and Williams [14], the effect of endothermicity, due to the high activation energy reaction C—CO_2, could be significant.

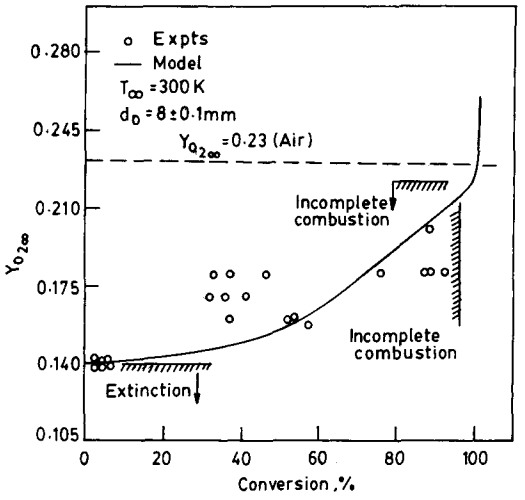

FIG. 5. Effect of ambient oxygen fraction on conversion at ambient temperature of 300 K.

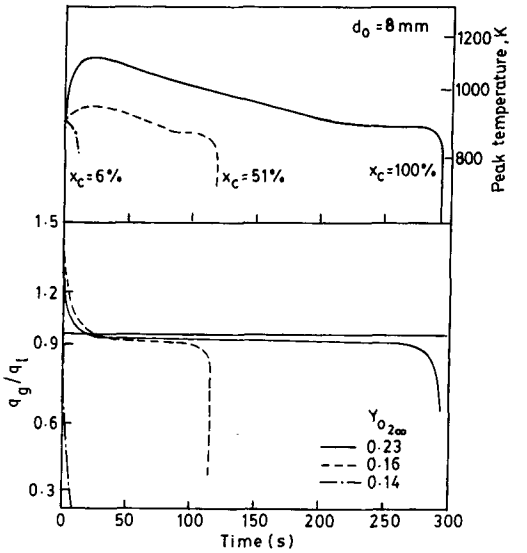

FIG. 6. Peak temperature and the ratio of the heat generation to the heat loss rate with conversion for different $Y_{O_{2\infty}}$.

Figure 5 shows the effect of ambient oxygen concentration on the conversion for an 8-mm-diameter char particle. In the experimental results mentioned earlier, it was found that below $Y_{O_{2,\infty}} = 0.21$ with N_2 being the diluent, the conversion was incomplete. It is seen from Fig. 5 that there is a gradual decrease in the percentage conversion with a reduction in $Y_{O_{2,\infty}}$. For ambient mass fractions of O_2 below 0.14, the conversion is less than 6%, thus indicating that the reactions are not self-sustaining below this oxygen fraction. This is interpreted as extinction. Similar results were obtained from the mathematical analysis for varying particle diameter, with extinction occurring at $Y_{O_{2,\infty}} = 0.14$. These results are consistent with those obtained by Rashbash and Langford [4] and Watson et al. [15] where combustion of wood and paper spheres were considered, respectively. It has been suggested that the planetary atmosphere should have a changing oxygen fraction during evolution and fire or its impossibility could be a strong agent of natural selection [16]. In this connection, the lower limit of oxygen fraction to sustain combustion ($Y_{O_{2,\infty}} = 0.14$) would be of interest.

Extinction is being caused by reduction in the particle diameter and by reduction in the ambient oxygen mass fraction. To understand the causes for extinction, an analysis of the heat generation and heat loss terms was carried out. The heat generation in the present context is the heat released due to char combustion, and the heat loss is the convective and radiative heat loss from the particle surface. With reduction in the initial particle diameter (d_0), toward the kinetic limit, the heat generation rate is proportional to the volume (d_0^3) and decreases faster than the heat loss rate, which is proportional to the surface area (d_0^2). This causes the extinction. Figure 6 shows the plot of peak temperature and the ratio of the heat generation to the heat loss rate with time for different cases of oxygen fraction. In all these cases, the initial temperature was set at 900 K. The peak temperature increases up to 1200 K before coming down somewhat linearly in time. An interesting feature of the plot is the sudden dip in temperature profile at 880 ± 20 K for all three cases considered. This temperature corresponds to the extinction condition. Calculations over a wider range of parameters confirmed the same temperature for extinction. For instance, in one numerical experiment, the initial temperature was set at 1000 K instead of 900 K for $Y_{O_{2,\infty}} = 0.14$. In this case, the temperature dropped sharply at 890 K after a 23% conversion, instead of a 6% conversion at 900 K. In all of the cases, the ratio of the heat generation to the heat loss rate is more than unity in the temperature rise region and below unity as conversion proceeds. It must be noted that during this period, the sphere is also decreasing in size. This extinction limit is similar to the stability limit obtained for the stirred reactor and discussed extensively in the combustion literature (chapters 6 and 16 of Refs. 17 and 18, respectively).

Results of the effect of flow velocities in the reactor chamber at 300 K of ambient temperature are presented in terms of $t_b/\rho d^{1.8}$ vs Re in Fig. 7. The results of conversion are also presented. The observed conversion is largely in excess of 90–93% in most cases. The predictions for the effect of velocity are carried out by augmenting the free convention with the forced convective heat and mass transfer. Two models for the presence of ash layer were in-

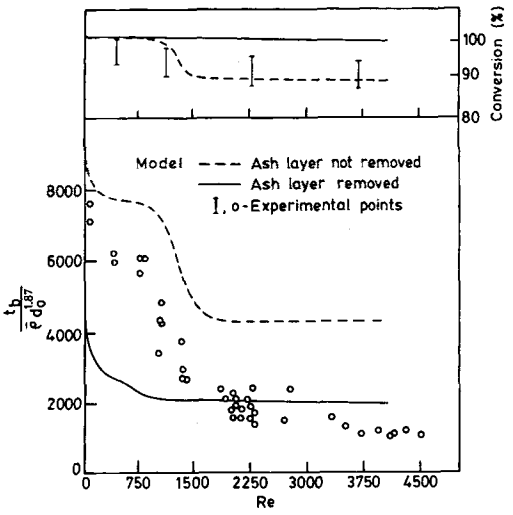

FIG. 7. The effect of Reynolds number on the conversion time of char spheres.

voked: (a) the ash layer is not removed, (b) the ash layer is continuously stripped away by the flowing gas. It was observed experimentally that beyond Re of 500, the ash layer was being blown away. (The predictions from these two models are described as (a) and (b).) Simulation of case (a) is performed by setting the sphere diameter at the initial value, and as reaction proceeds, more and more of the outer layer will become inert. Case (b) is simulated by taking the sphere diameter as reducing with time, since the material in the outer part gets consumed by reaction. The experimental results fall between the limits of cases (a) and (b). They are more close to limit (a) at lower Re and close to limit (b) at higher Re. Even so, the conversion results are close to model (a); model (b) predicts conversion close to 100%. This is possibly because of the additional heat loss to the wire basket, which becomes important only toward the end of conversion. Perhaps with increasing Re, the amount of ash being removed due to flow effects is also increasing, reaching a limit at around Re = 2000. The reduction in burn time around Re = 500, both in the experiments and the model, is consistent with the results obtained by Kuwata et al. [3] on the paper spheres. The increase in burn time beyond Re of 500 observed in Kuwata et al. has not been observed here either experimentally or from the model.

Conclusions

The experimental and modeling aspects related to the combustion of char in an ambient atmosphere with varying oxygen concentration has been discussed in this paper. The conversion time dependence for the char oxidation was shown to be $t_b \sim d_0^n$, where $n = 1.9$ and 2.0 for combustion at $T \sim 300$ and 1000 K, respectively, for particle diameters above 1 mm. The importance of conductivity of char and the C + CO_2 reaction during char combustion was brought out. For the range of the present study, the C + CO_2 reaction was not essential to explain the observed peak temperatures and burn times. Extinction of particle during combustion occurred at an ambient oxygen mass fraction of 0.14 for $T \sim 300$ K. The extinction of the char particle and incomplete combustion were shown to be due to the heat loss rate dominating the heat generation.

Nomenclature

d_0	initial diameter (m)
D	diffusion coefficient (m^2/s)
$\bar{D}$	effective diffusivity (m^2/s)
ε	porosity
$E_{1,2}$	activation energy (Eqs. (8) and (9)) (kJ/mol)
H_C	heat of combustion of carbon (MJ/kg)
$k, k_c, \bar{k}$	thermal conductivity of gas, carbon, and porous char (W/m K)
M_i	molecular weight of species i (kg/mol)
Nu	Nusselt number
p	pressure (Pa)
q_g, q_l	heat generation and heat loss rates (W)
r	radial coordinate (m)
r_p	pore radius in char (m)
R	universal gas constant (J/kg mol K)
S_g	surface area per unit mass of the char (m^2/kg)
t	time (s)
$\dot{R}''$	radiation flux (W/m^2)
$S_{1,2}$	rate constants of Eq. (7)
T	temperature (K)
Y_i	mass fraction of species i
k_1–k_4	rate constants of Eq. (10)
x_c	conversion
X_{OS}	mole fraction of oxygen at surface
ρ	density of gas (kg/m^3)
$\dot{\omega}_i'''$	volumetric reaction rate of Eq. (4) (kg/m^3 s)

REFERENCES

1. Laurendeau, N. M., *Prog. Energy Combust. Sci.* 4:221 (1978).
2. Mukunda, H. S., Paul, P. J., Shrinivasa, U., and Rajan, N. K. S., *Twentieth Symposium (International) on Combustion*, The Combustion Institute, Pittsburgh, 1984, pp. 1619–1628.
3. Kuwata, M., Stumbar, E., and Essenhigh, R., *Twelfth Symposium (International) on Combustion*, The Combustion Institute, Pittsburgh, 1969, pp. 663–674.

4. Rashbash, D. J., and Langford, B., *Combust. Flame* 12:33–40 (1968).
5. Simmons, W., and Ragland, K., *Combust. Sci. Technol.* 46:1–15 (1986).
6. Dasappa, S., Paul, P. J., Mukunda, H. S., and Shrinivasa, U., *Chem. Eng. Sci.* 49 (2):223–232 (1994).
7. Howard, J. B., *Combustion of Carbon with Oxygen*, Technical Report, MIT, 1967.
8. Smith, I., and Tyler, R., *Combust. Sci. Technol.* 9:87–94 (1974).
9. Blackwood, J. D., and Ingeme, A. J., *Aust. J. Chem.*, 13:194–209 (1960).
10. Anon. *Gas Engineers' Handbook*, McGraw Hill Book Co. Inc., New York, 1934.
11. Goldman, J., Xieu, D., Oko, A., Milne, R., and Essenhigh, R. H., *Twentieth Symposium (International) on Combustion*, The Combustion Institute, Pittsburgh, 1984, pp. 1365–1372.
12. Groeneveld, M. J., and van Swaaij, W. P. M., *Chem. Eng. Sci.* 35:307–313 (1980).
13. Groeneveld, M. J., *The Co-Current Moving Bed Gasifier*, Ph.D. Thesis, Twente University of Technology, Netherlands, 1980.
14. Ubhayakar, S. K., and Williams, F. A., *J. Electrochem. Soc. (Solid State Sci. Technol.)* 123(5):747–756, (1976).
15. Watson, A. J., Lovelock, J. E., and Margulis, L., *Biosystems* 10:293–298 (1978).
16. Robinson, J., *Paleogeogr. Paleoclimatol., Paleoccol. (Global Planet. Change Sect.* 75:223–240 (1989).
17. Vulis, L. A., *Thermal Regimes of Combustion*, McGraw Hill, New York (1961).
18. Spalding, D. P., *Combustion and Heat Transfer*, Oxford Pergamon Press, New York, 1979.

COMMENT

Reginald E. Mitchell, Stanford University, USA. You found that your wood-char spheres burned with decreases in diameter, diameter changing with burnoff to the 1.87 power. One would expect that for diffusion-limited burning, diameter would vary with burnoff to the second power (i.e., the d^2 power law dependence). Since mass equals density times volume, if the d^2 power law dependence is not observed, then density must decrease with mass loss. In your calculations of burning times, you assumed that density was constant. Constant-density diffusion-limited burning requires a d^2 dependence of diameter with mass loss, otherwise mass is not conserved. Would you comment on this apparent discrepancy? Might it be possible that your wood-char spheres burned along grains and that particle shape was changing during mass loss, the particles becoming more like prolate spheroids? Such behavior would support a power dependency less than 2.

Author's Reply. It is true that the theory for a constant-density diffusion-limited situation produces a d^2 dependence on burning time. However, our theory assumes neither constant density nor diffusion limitedness. The heat and mass flux in the gas phase are modified by free convection, which is also taken into account in the theory. The exponent of 1.87 is obtained as a net effect of all these factors. From the result obtained on the burning time for varying diameters, we concluded that the situation is close to diffusion-limited conditions.

The exponents are 1.87 and 2.0 for ambient temperatures of 300 and 1000 K respectively. The difference is explained due to differences in mass transfer caused by free convection for the low ambient temperature. The result is further substantiated by the observation (not presented in the paper) that the reaction rate is limited to one cell close to the surface, and hence combustion proceeds virtually by the shrinking core mechanism.

Partially burnt char was examined and no significant ovality was found. Since the initial porosity was large, the resistance offered by pores to diffusion was small in all cases studied. Hence the diffusivities along and across the grains are almost the same.